Preparation and characterization of α-Fe nanowires located inside double wall carbon nanotubes

Jose Jorge [a], Emmanuel Flahaut [b], Fernando Gonzalez-Jimenez [a,*], Gema Gonzalez [c], Jesus Gonzalez [d], Edgar Belandria [d], Jean M. Broto [e], Bertrand Raquet [e]

[a] Laboratorio de Magnetismo, Fisica, Ciencias, Universidad Central de Venezuela, Caracas, Venezuela
[b] CIRIMAT, Université Paul-Sabatier, UMR CNRS 5085, 31062 Toulouse cedex 4, France
[c] InstitutoVenezolano de Iinvestigaciones Científicas- IVIC, Caracas, Venezuela
[d] Centro de Estudio de Semiconductores, Universidad de los Andes, Merida, Venezuela
[e] Laboratoire National des Champs Magnétiques Pulsés, UMR 5147 CNRS-UPS-INSA, Toulouse, France

A B S T R A C T

Capillary effect was used to fill double wall carbon nanotubes (DWCNT) with iron. The samples are characterized by Mössbauer and Raman spectroscopies, TEM, SAED, and magnetization. The experimental results indicate the presence of α-Fe nanowires inside the DWCNTs. The samples are ferromagnetic at room temperature. There are three striking results due to the confinement effects on the physical behavior of α-Fe: the hyperfine fields increase, the Debye temperature decreases and Raman modes are observed.

1. Introduction

Aiming at using the CNTs as a nanohost to template the growth of one-dimensional objects, numerous authors have tried to fill carbon nanotubes, firstly MWCNTs [1–5], then SWCNTs [6,7], with transition ferromagnetic metals, e.g. Fe, Co, Ni. In the case of iron filling, ferrocene was used as iron source, which was subsequently reduced at rather high temperatures, 850 °C–1050 °C. As a result a mixture of cementite, γ-Fe and α-Fe was obtained [2–4]. Other groups have reported Fe filling, but without clearly specifying its nature [6,7]. More recently, a clear evidence of the presence of α-Fe in MWCNTs of 20–25 nm, starting with ferrofluids (10 nm magnetite particles) was reported [5]. In this work, we have followed a novel approach [8] to the filling of DWCNTs in which the external wall protects the internal one, which maintains its structure and chemical and physical properties. This fabrication process uses the capillary effect to achieve the filling of the nanotubes. In practice, the DWNT is placed in an aqueous solution of an iron precursor which is adsorbed in the hollow internal tube [7].

Our work may prove relevant in paving the road for the advanced use of Fe-filled DWCNTs as functional materials for sensing and electronic devices which could combine the advantages of charge and spin electrons for transport.

2. Experimental

DWCNTs, were produced by Catalytic Chemical Vapour Deposition (CCVD) from a H_2–CH_4 mixture (18 mol% CH_4, heating and cooling rates 5 °C/min, maximun temperature 1000 °C, no dwell) using oxide (Mg, Co, Mo)O catalysts [9]. The pristine CNTs contained ca. 75% DWCNTs, with 1.5 nm average internal diameter and 2.2 nm average external diameter. The CNTs were filled with iron by using a simple method based on the capillary filling with an $FeCl_3$ solution (adapted from [7]). To open the CNTs around 80 mg were placed in 50 ml of 2 M HNO_3, and refluxed for 30 h ca. 130 °C. The sample was filtered and washed with deionised water, and then placed in a highly concentrated $FeCl_3$ aqueous solution (ca. 9 mol L^{-1}) and sonicated for 30 min. [7] The suspension was then stirred for 48 h at room temperature, and let to rest for 25 days. In order to remove the $FeCl_3$ that could be present outside the tubes the suspension was filtered and quickly washed with distilled water. The sample was dried overnight at 80 °C. Finally, the sample was heated up to 320 °C for 1 h in a flow of Ar, to decompose $FeCl_3$ into Fe and Cl [7]. The process was completed by heating at 650 °C in a flow of H_2 to reduce the oxides which could be present.

For the characterization of the Fe@DWCNTs we adopted the following procedure:

- To identify the state of iron we used Mössbauer Spectroscopy (MS) at the 14.4 keV transition of ^{57}Fe, with a ^{57}Co in Rh source. The spectrometer is a homemade combination of a driver, Multi-Channel Scaling system (MCS) and nuclear detec-

* Corresponding author. Fax: +58 2126051675.
E-mail address: fgonzale@fisica.ciens.ucv.ve (F. Gonzalez-Jimenez).

doi:10.1016/j.cplett.2008.04.019

tion chain with a proportionnal counter. The spectrometer was run in the triangular symmetric mode and calibrated with bulk α-Fe. The spectra were fitted with lorentzian shapes for the lines and a limited number of free parameters for each subspectrum, e.g. isomer shift(IS, relative to α-Fe), HWHM (GA), quadrupole splitting (QS) and the hyperfine field (HPF).

- The morphological and structural analysis of the sample was carried out using a combination of Transmission Electron Microscopy (TEM) at different levels of resolution, TEM (JEOL JEM 1011), HRTEM (JEOL JEM 2100F), and Scanning Area Electron Difraction SAED (Phillips CM 120).
- Raman spectra of the DWNTs were recorded in the back-scattering geometry using a micro-Raman, triple grating system (DILOR XY800) equipped with a cryogenic CCD detector. The spectral resolution of the system was about 1 cm^{-1}. For excitation, the 514.5 nm line of an argon laser was focused on the sample by means of a 100X objective, while the laser power was kept below 2 mW, in order to eliminate laser-heating effects on the probed material and the concomitant softening of the observed Raman peaks. The phonon frequencies were obtained by fitting Lorentzian functions to the experimental peaks.
- Magnetization Measurements Vibrating Sample Magnetometer (VSM) with a conventional coil, maximum field inmersed in liquid nitrogen 0.32 T.

3. Results and discussion

A TEM analysis of the sample gave us the first indications of filling of the DWCNTs with iron. The electronic state of iron was characterized using ^{57}Fe Mössbauer spectroscopy. In Fig. 1a the room temperature spectrum indicates the predominant presence of the characteristic sextet of α-Fe (∼95%) and a small contribution of a doublet, attributable to a superparamagnetic oxyde(∼5%). This is confirmed by observing the spectrum at 47 K in Fig. 1b, where in addition to the α-Fe spectrum, a slow relaxation magnetic spectrum due to the small superparamagnetic particles can be seen particularly by the presence of weak broad lines at high velocities(at app. +8, −8 cm/s). The fittings give for 1a) HPF = 34.4 ± 0.1 T (average of a HPF distribution) with QS = 0.0 mm/s and IS = 0.0 mm/s, in agreement with the α-Fe values, except the HPF which is increased by ∼4% with respect to the bulk metallic Fe (33.0 T), and for 1b) at 47 K, HPF = 35.2 ± 0.1 T (average of a HPF distribution), QS = 0.0 mm/s and IS = 0.12 mm/s, for α-Fe (here also increased with respect to bulk iron, 33.6 T, ∼5%), and for the oxyde HPF = 50.5 ± 0.5 T (average of a HPF distribution), QS = −0.2 and IS = 0.54 mm/s. We interpret these values as corresponding to small particles of hematite (α-Fe_2O_3). It is remarkable that in this work we obtained almost only α-Fe, whereas other authors obtained cementite (Fe_3C, 20%), γ-Fe (32%) and α-Fe (48%) in samples of Fe@MWCNTs prepared usign other preparation techniques [2–4]. We attribute the significant increase of the hyperfine field corresponding to α-Fe to confinement effects. The bcc structure of bulk α-Fe is modified in nanotubes as suggested by theoretical calculations for SWCNTs filled with iron. These calculations indicate that while the bcc Fe structure is still the lowest energy one, it is relaxed with the (110) direction parallel to the nanotube axis [10]. The same calculations give larger magnetic moments than in the bulk, which is in line with the increase in the hyperfine field. The very mild method used to introduce Fe in the interior of the nanotube, based in the capillary action, suggests that the iron atoms find place in a relaxed bcc structure. In this direction it is worth saying that when the bulk iron is subjected to hydrostatic pressures, i.e. the cell parameter decreases, the hyperfine field decreases [11]. On the other hand the increase in the cell parameter as a result of the relaxation of the structure decreases the forces between iron atoms and in consequence the Mössbauer absorption *f* factor should decrease. This is observed by measuring the thermal evolution of the absorption on the iron spectrum, which leads to an apparent calculated Debye temperature $\theta_D \sim 240$ K, considerably lower than in the bulk case where $\theta_D \sim 470$ K (An extensive study of the thermal behavior and the corresponding calculated results will be published elsewhere.).

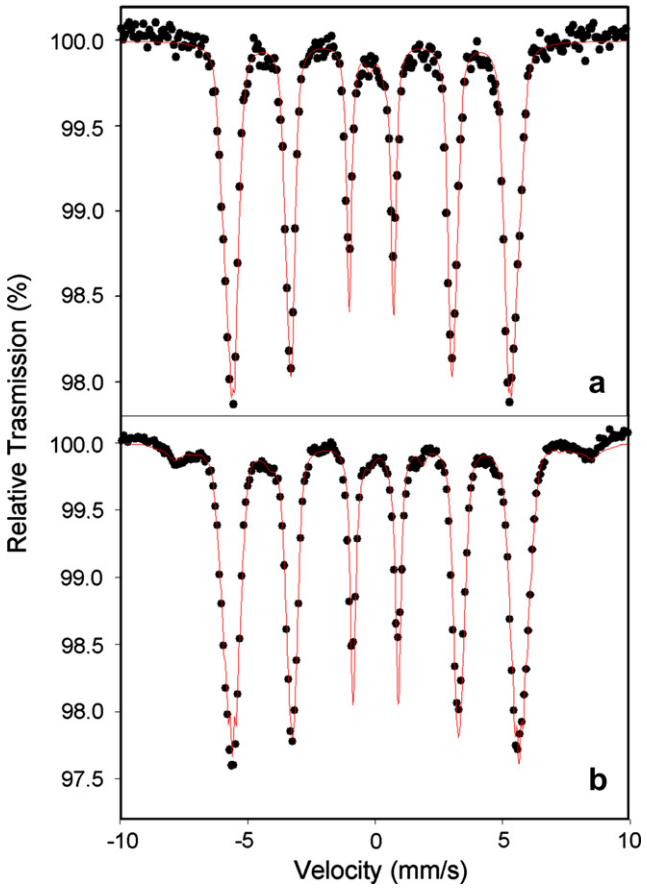

Fig. 1. Mössbauer spectra of the Fe@DWCNTs at 293 K (a) and 47 K temperatures (b).

Fig. 2 displays images of isolated filled nanotubes obtained using various techniques. In Fig. 2a the HRTEM image indicates the presence of an open DWCNT filled in the interior (d_{int} = 1.5 nm), with a material whose identity is consistent with the Mössbauer spectrum that seems to correspond to α-Fe. In the external part (d_{ext} = 2.2 nm) we can see some adherences which also can be assumed to be part of the oxide observed by Mössbauer. In Fig. 2b there are at least two bundles between which there are three isolated nanotubes, where two of them are open and filled up to 13 nm and 30 nm lengths, respectively, while the third one shows a filler of 40 nm approximately with an aspect ratio of 54.

Fig. 3a shows three bundles in three different directions and also a partial view of an isolated nanotube. In the lower part of the figure the bundle observed has a diameter d_B = 12 nm, which in the two dimensional packing hexagonal model [12] could correspond to 40 DWCNTs. Due to the difficulty to make the SAED study on one isolated nanotube, we decided to focus the electron beam in the region of the bundles shown in Fig. 3a.

In Fig. 3b there are two rings corresponding to α-Fe, the (110) and the (200). Those rings are non continuous indicating that there

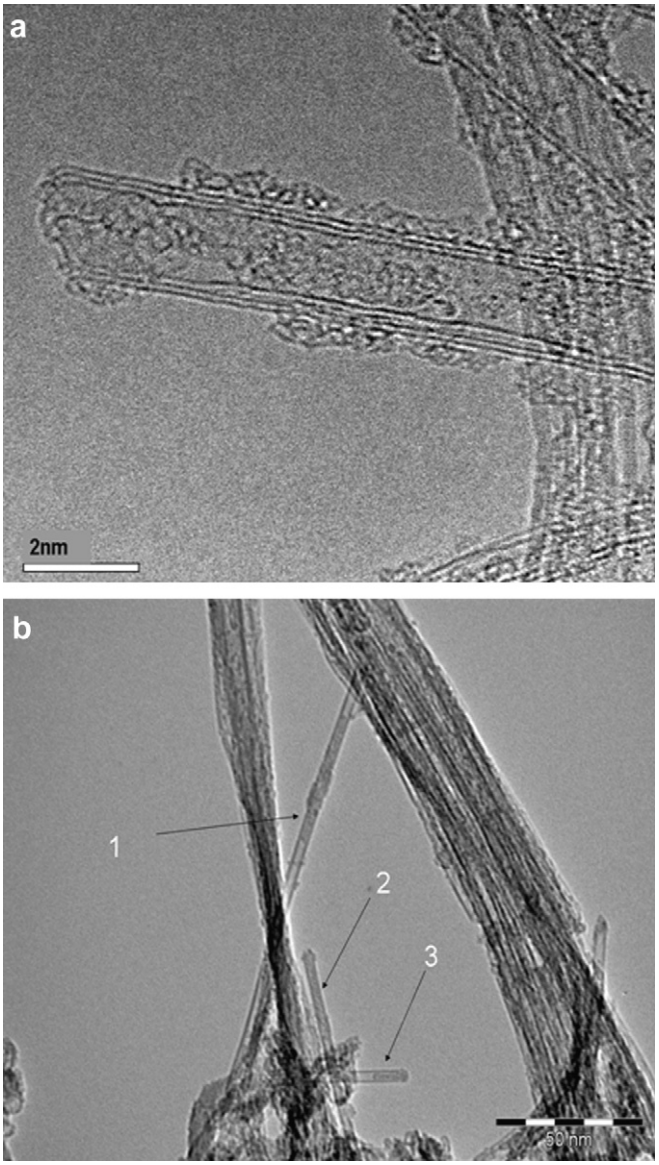

Fig. 2. HRTEM image of an open filled DWCNT (a), two bundles between which there are three isolated nanotubes: (1) filled 40 nm, (2) open and filled 30 nm and (3) open and filled 13 nm (b).

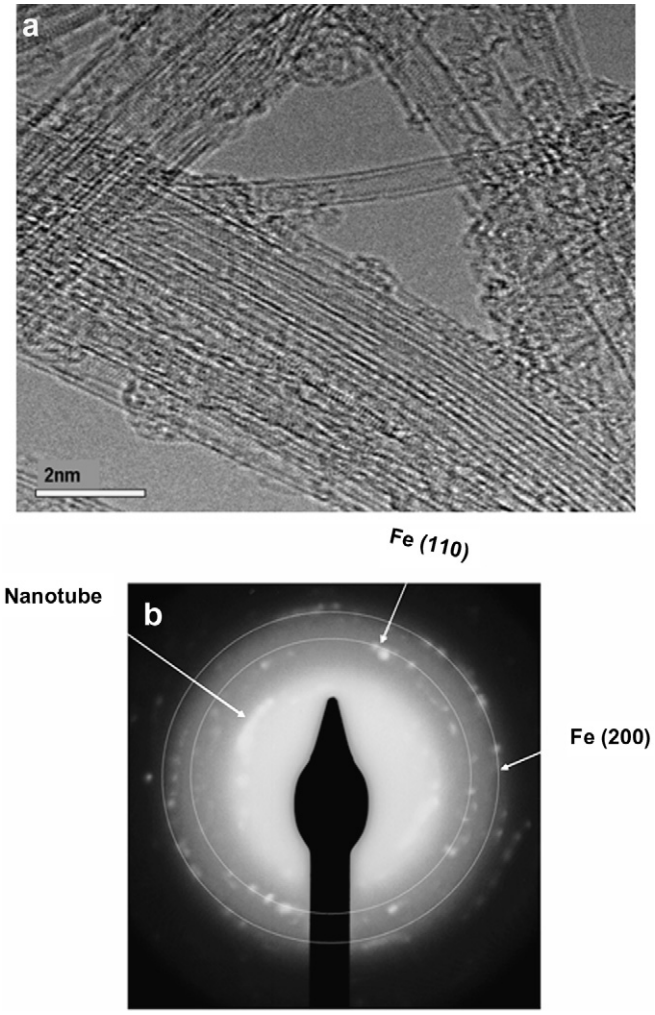

Fig. 3. HRTEM image of the bundles (a), and corresponding Selected Area Electron Diffraction pattern showing reflexions of both the CNT and α-Fe (b).

are preferential orientations of the Fe nanowires. We also indicate reflections (002) due to the DWCNTs ('nanotube' in the figure), corresponding to the intergraphene distance $d = 3.37$ A of the two graphene layers of the double wall (here also the preferential orientations mentioned above are clear).

To further characterize the samples of Fe@DWCNTs, we undertook a Raman Spectroscopy study. Even if bulk α-Fe (bcc) is not Raman active, i.e. does not show optical phonons (all the branches are acoustical), if the periodicity of the crystal lattice is interrupted, as is the case for nanowires, then the q-vector selection rule is relaxed. As a consequence, overtones of acoustic phonons ($2TA_1$ and $2TA_2$) of the Brillouin zone border are observed (Γ-N direction of the Brillouin zone) [13]. The values of observed frequencies are shifted compared to those obtained in the two-phonons density of acoustic states for α-Fe. The combinations of Fe phonons are placed in the frequencies range of the nanotubes radial breathing modes (RBM), but as they are combination modes they are distinguished because they are wider than the radial ones. The frequencies involved are to be found between 125 cm^{-1} and 325 cm^{-1} [13,14], and are in good agreement with Raman measurements on α-Fe nanowires embedded in MWCNTs [15].

In Fig. 4 we present the experimental Raman spectra. Fig. 4a shows the tangential modes and the D band which correspond to the double resonance induced by the defects in the carbon nanotubes. Table 1a reports the values of the centroids and widths of the fitted lorentzian lines.

The high value of the ratio of the intensities of the tangential external mode and the D band, indicate that the crystalline quality of the nanotubes is rather good. Also the larger intensity of the external mode with respect to the internal one, indicate that in this sample the chiralities correspond predominantly to semiconductor nanotubes, with an important concentration of metallic ones, as confirmed by the presence of the band observed around 1508 cm^{-1}. The frequencies of the tangential modes of the DWCNTs are red shifted compared with the values of the empty ones and this effect is attributed to the charge transfer between the iron nanowire and the inner wall of the CNT [15].

Fig. 4b shows the radial breathing modes (RBM) spectral region, corresponding to outer and inner NTs of the DWCNTs (diameters ranging from 0.9 nm (inner) to 2.2 nm (outer)). Also the acoustical modes from the α-Fe nanowires are observed. Table 2 show the frequencies and the FWHM of the lorentzian fitted lines attributed to the RBM modes, as well as the calculated chiralities and diameters [16]. In the insert we compare the inner RBM of

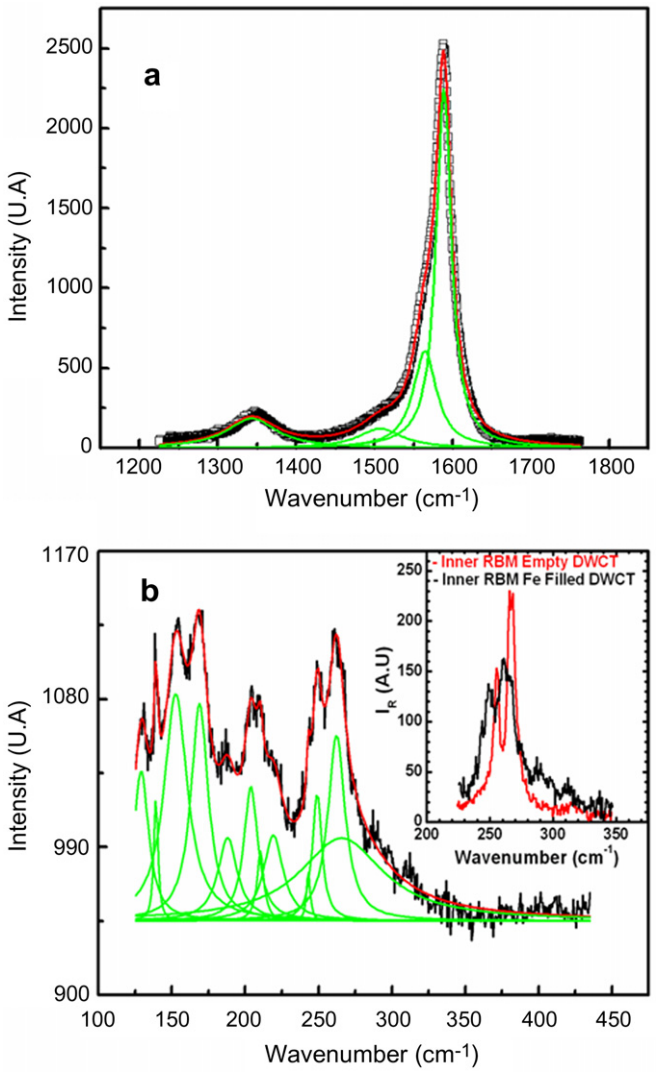

Fig. 4. Raman spectrum from a 514 nm laser: tangential modes of the inner and outer filled DWCNTs (right) and D band region (left) (a), radial breathing modes (RBM) of the inner and outer filled DWCNTs (b). In the insert we compare the inner RBMs of the empty and filled DWCNTs. Solid green lines are the fits by Lorentzians. (For interpretation of the references to colour in this figure legend, the reader is referred to the web version of this article.)

Table 1
Fe at DWCNTs frequencies and FWHM of phonons in the tangential modes region

Wave number (cm^{-1})	Width
1343.6 ± 0.5 (D)	78 ± 2
1508 ± 1 (metallic)	68 ± 4
1564.4 ± 0.3 (internal)	37 ± 1
1588.45 ± 0.04 (external)	23.6 ± 0.1

the empty and filled DWCNTs. As observed filling the inner tubes with iron produces a broadening and a red shift in the RBMs, this is because the frequencies of the acoustical modes of the α-Fe nanowire are in the same spectral domain.

These measurements confirm the presence of α-Fe (bcc) in a confined situation.

In Fig. 5, the hysteresis loop observed at room temperature indicates that the sample of Fe @ DWCNTs is ferromagnetic, showing a coercive field of H_C = 190 G and a remanence M_R = 0.02 emu, indicating a high magnetic stability. As pointed out above, our SAED

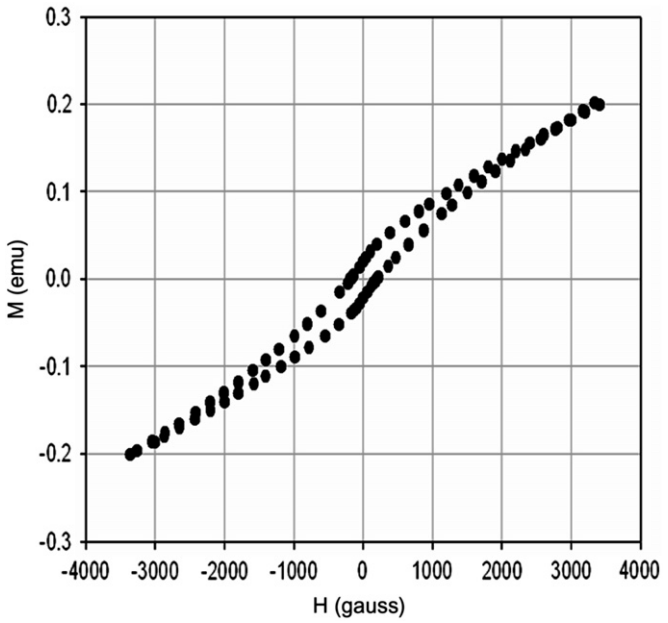

Fig. 5. The magnetic hysteresis measurements with a VSM at 300 K.

Table 2
The diameters are calculated from the 1/D dependence radial modes frequencies, as well as the chiralities

Wave number (cm^{-1})	Width	Assignments (n,m)	Diameter (n,m)
129.1 ± 0.3	12 ± 1	(21,8)	1.939
139.1 ± 0.1	3.4 ± 0.5	(21,5)	1.863
152.6 ± 0.3	19 ± 1	(21,1)	1.678
168.9 ± 0.2	14 ± 1	(13,9)	1.495
187.9 ± 0.6	16 ± 3	noise	
203.8 ± 0.6	12 ± 2	(11,7)	1.228
210.3 ± 0.5	6 ± 2	(12,5)	1.182
219.1 ± 1.0	16 ± 4	(14,1)	1.135
243.1 ± 0.3	3 ± 1	(13,0)	1.017
249.0 ± 0.3	8 ± 1	Fe-bcc	
262.3 ± 0.2	14 ± 1	(12,0)	0.939
266 ± 4	70 ± 8	Fe-bcc	

and HRTEM results show that we have preferential orientations in the bundles, and that the ensemble of bundles is randomly distributed in all directions. The ferromagnetic behavior is consistent with the observed fact that after the sample is magnetized, an important fraction of the nanowires conserves its magnetization, and this leads to the observed remanence and coercive field. It is also clear from the Mössbauer result that at room temperature no trace of superparamagnetism is present in those samples, even though this is a nanostructured α-Fe system. There must be at least two reasons to maintain the magnetization of these nanowires in one direction: the shape anisotropy and the magnetic surface effects [7,17].

4. Conclusion

In first instance the adopted chemical wetting method was successful, as reported by other authors [7] for SWCNT's, but here iron entered almost all as α-Fe inside DWCNT's.

In the fundamental aspects, the relaxation of the iron atoms due to the confinement have two consequences: the increase of the hyperfine magnetic field and the softening of the bcc lattice.

For the applications, the fact that α-Fe is in the form of nanowires with big aspect ratios, and also have striking ferromagnetic properties at room temperature, make this materials promissing for magnetic probes, AFM tips, memories, nanodevices for spin electronics, functionalized magnetic materials for biomedical applications.

Acknowledgements

This work was undertaken in the frame of the Franco-Venezuelan Cooperation Program PCP 'Nanotubos de Carbono'. Critical reading by Prof. V. Mujica is kindly appreciated. P. Landois and L. Datas are aknowledged for help with TEM characterization of the samples (TEMSCAN, Université Paul Sabatier).

References

[1] N. Grobert et al. , Appl. Phys. Lett. 75 (1999) 3363.
[2] J.F. Marco et al. , Hyperfine Interact. 139/140 (2002) 535.
[3] T. Ruskov et al. , J. Appl. Phys. 96 (12) (2004) 7514.
[4] V. Pichot, P. Launois, M. Pinault, M. L'Hermite, C. Reynaud, Appl. Phys. Lett. 85 (3) (2004) 473.
[5] D. Jain, R. Wilhelm, Carbon 45 (2007) 602.
[6] Y. Li, R. Hatakeyama, T. Kaneko, T. Okada, Jpn. J. Appl. Phys. 45 (15) (2006) L428.
[7] E. Borowiak-Palen et al. , Chem. Phys. Lett. 421 (2006) 129.
[8] Y.F. Li, R. Hatakeyama, T. Kaneko, T. Izumida, T. Okada, T. Kato, Nanotechnology 17 (2006) 4143.
[9] E. Flahaut, R.Bacsa.A.R. Bacsa A.. Peigney, C. Laurent, Chem. Commun. (2003) 1442.
[10] M. Weissmann, G. Garcia, M. Kiwi, R. Ramirez, C.C. Fu, Phys. Rev. B 73 (2006) 125435.
[11] R.D. Taylor, M.P. Pasternak, J. Appl. Phys. 69 (8) (1991) 6126.
[12] J.M. Cowley, P. Nikolaev, A. Thess, R.E. Smalley, Chem. Phys. Lett. 265 (1997) 379.
[13] S. Klotz, M. Braden, Phys. Rev. Lett. 85 (2000) 3209.
[14] X. Sha, R.E. Cohen, Phys. Rev. B 73 (2006) 104303.
[15] E. Belandria, Doctoral Dissertation, ULA, Merida, Venezuela 2008 (February).
[16] M.S. Dresselhauss, P.C. Eklund, Adv. Phys. 49 (6) (2000) 705.
[17] A.H. Morrish, The Physical Principles of Magnetism, John Wiley & Sons Inc., 1965.